

# 50+ Years of Intrinsic Breakdown

**Key words:** intrinsic breakdown, computational quantum mechanisms, DFT, DFPT

## Introduction

The story of intrinsic dielectric breakdown in a modern context starts around 1930, when researchers such as von Hippel, Zener, and Fröhlich started to explain electrical breakdown, first using semi-classical theories and eventually using quantum mechanics. Von Hippel “got it right,” and implementation of his ideas using modern computational quantum mechanics provides an excellent estimate of intrinsic breakdown, as shown in this article. Between von Hippel’s early work and present implementations using computational quantum mechanics, a number of semiempirical approaches were implemented, some of which provided excellent agreement with measured data over their limited range of applicability.

Intrinsic breakdown refers to the electric field which will cause breakdown of a “perfect” material in a very short time, i.e., without the effects of high field aging. The measurement of intrinsic breakdown is always problematic, as “perfection,” even in crystalline materials, is difficult to achieve on a macroscopic basis. Electrode–material interfaces are never “perfect,” and, in principle, the position of the electrode Fermi level within the band gap and relative to impurity states can affect the breakdown field. Thus when metallic electrodes are employed, many tests must be carried out, and the intrinsic breakdown field is taken as the upper limit of the experimental data. More recently, intrinsic breakdown has been measured using an intense optical field, which, for transparent materials, avoids electrode effects. The electric field of electromagnetic radiation can be related to its energy density ( $J/m^3$ ) by the energy density of an electric field,  $\epsilon E^2/2$ , where  $E$  is the optical electric field and, for an optical field,  $\epsilon$  is the electronic component of the material dielectric constant, typically about  $20 \times 10^{-12}$  F/m (relative electronic dielectric constant of about 2.2), which results in an index of refraction of  $n = \sqrt{2.2} = 1.5$ . The power (W) or intensity ( $W/m^2$ ) of a laser can be related to the energy density ( $ED$ ,  $J/m^3$ ) through (1)

$$ED_{\text{optical}} = \frac{Pn}{cA} = \frac{In}{c}, \quad (1)$$

The second of a series of invited reviews to be published during 2013 to mark the 50th anniversary of DEIS.

## Ying Sun

*Institute of Materials Science, University of Connecticut, Storrs, CT 06269, USA*

## Clive Bealing

*Institute of Materials Science, University of Connecticut, Storrs, CT 06269, USA*

## Steven Boggs

*Institute of Materials Science, Departments of Physics and Electrical Engineering, University of Connecticut, Storrs, CT 06269, USA*

## Ramamurthy Ramprasad

*Institute of Materials Science, Departments of Physics and Materials Science and Engineering, University of Connecticut, Storrs, CT 06269, USA*

*The quantum mechanical basis of intrinsic breakdown was set out in the 1930s, but only recently can we implement these ideas accurately, from first principles.*

where  $P$  is the power of the laser (W),  $I$  is intensity ( $\text{W}/\text{m}^2$ ),  $n$  is the index of refraction of the dielectric,  $c$  is the speed of light in vacuum, and  $A$  is the area to which the optical beam is focused. If we equate this to the energy density from the electric field, we arrive at (2)

$$E_{\text{optical}} = \sqrt{\frac{2P}{\varepsilon_0 c A n}} = \sqrt{\frac{2I}{\varepsilon_0 c n}}. \quad (2)$$

A 100-kW pulsed laser focused to an area of  $10^{-10} \text{ m}^2$  can achieve an electric field in the range of 700 kV/mm, with the field increasing as the square root of the power. By focusing a pulsed laser into a transparent dielectric sample, the laser power (electric field) at which the sample is damaged can be determined by applying successively greater power pulses and inspecting the sample after each pulse. This approach allows a small volume to be tested, which minimizes the likelihood of defects, and avoids electrode effects. Most such data have been generated with  $\text{CO}_2$  lasers ( $10.6 \text{ }\mu\text{m}$ ) or YAG lasers ( $1.06 \text{ }\mu\text{m}$ ). The period of the light is given by  $\tau = \lambda/n/c$ , where  $\lambda$  is the wavelength. Thus for  $10.6\text{-}\mu\text{m}$  radiation in a medium with  $n = 1.5$ , the period is about 50 fs ( $50 \times 10^{-15} \text{ s}$ ) while for  $1.06\text{-}\mu\text{m}$  radiation, the period would be an order of magnitude shorter, at about 5 fs. Under high electric field conditions, in which an electron gains energy from the electric field and loses energy to the “lattice” (phonons), an electron has a characteristic time constant for coming to equilibrium. To first order, this can be taken as the mean time between electron–phonon scattering events which are likely to change both the energy and momentum (direction) of the electron. If the optical period is short compared to the mean time between scattering events, the reversal of the optical field between scattering events tends to reduce the energy transferred from the field to an electron. If the optical period is long compared to the mean time between scattering events, then the electric field is “quasistatic” in the context of scattering events, and the electric field for optically induced breakdown will be similar to the dc breakdown field. As will be shown below, the mean time between electron–phonon scatter events is sufficiently short that optically induced breakdown, even at  $1.06 \text{ }\mu\text{m}$ , should be very close to the dc value.

In addition to laser-based measurements of transparent bulk materials, a great deal of work has been published on breakdown of thin  $\text{SiO}_2$  films as related to gate oxides, some of which addresses intrinsic breakdown [1]. Since the thin films are usually part of electronic devices, current–voltage characteristics can be measured, and breakdown fields can also be measured relatively easily.

## Historical Overview of Intrinsic Breakdown Theory

In 1932, von Hippel [2] postulated that breakdown occurs when the “average electron” gains energy more rapidly from the electric field than it loses energy to the lattice (i.e., to phonons) for all electron energies less than that needed to produce impact ionization, which is often called von Hippel’s low energy criterion for breakdown [3]. Von Hippel explained breakdown theory

qualitatively, e.g., he did not give an expression for the electron–lattice collision rate or electron energy loss rate.

Zener’s field emission theory (1934) proposed an alternative mechanism which assumes that breakdown occurs as a result of field emission, e.g., that in an electric field, electrons can tunnel from the valence band to the conduction band without changing energy [4]. He also derived an expression for the probability that an electron will make a transition to the conduction band; however, Zener’s approach is not consistent with the temperature dependence of the intrinsic breakdown field [5].

In 1937 Fröhlich [6] proposed a theory of intrinsic breakdown based on impact ionization which differs from von Hippel’s approach primarily in the condition postulated for breakdown. Fröhlich postulated that breakdown occurs when the electric field is sufficiently large that electrons in the high energy tail of the electron energy distribution, which have sufficient energy to cause impact ionization, gain more energy from the field than they lose to phonons (Fröhlich’s high energy criterion). Fröhlich made a quantitative calculation of the breakdown field which assumes that only longitudinal optical phonons interact with electrons. His calculation is based on a quantum mechanical derivation of the electron relaxation time. Both von Hippel and Fröhlich neglect the interaction of electrons with nonpolar (i.e., acoustic and transverse optical phonon) modes of vibration.

In 1981, Sparks [7] proposed a breakdown model based on analytical approximations which agrees well with experimental laser breakdown data, including the magnitude and temperature dependence of the breakdown field, pulse-duration dependence, material dependence, and wavelength dependence. The good agreement with measured breakdown field is the result of more realistic electron–phonon scattering rates used in his calculation, e.g., both acoustic and optical phonons are included. Quantitative calculations of breakdown field by both Fröhlich and Sparks were performed only for alkali halides, since the simple structure of these materials eases the derivation of analytical solutions.

In 1994, D. Arnold from IBM presented a detailed theoretical study of impact ionization related to transport phenomena in  $\text{SiO}_2$  thin films [1], in which the Boltzmann transport equation is integrated with the Monte Carlo method using electron–phonon scattering rates derived from photo-induced electron transmission experiments. The study shows that acoustic phonon scattering accounts for the high energy tail in the electron energy distribution, and breakdown in  $\text{SiO}_2$  thin films might be caused by the cumulative degradation of the thin film structures near interfaces, primarily by hot electron–induced hydrogen chemistry. In the last few years [8]–[10], first principles quantum mechanical methods for calculation of electron–phonon scattering rates have been pursued. Development of the intrinsic breakdown theory is summarized in Table 1.

## Avalanche Breakdown Theory

Most theories of intrinsic breakdown start from the hypothesis of an electron avalanche [2], [3], [6], [7], [13]. The general features of electron avalanche breakdown theory include the acceleration of a conduction electron by the electric field, the loss of energy from electron to phonons, the generation of a second conduction electron accompanied by a loss of kinetic energy of

**Table 1. Summary of Theories of Intrinsic Breakdown.**

Year	Contributor	Materials	Brief description
1932	Von Hippel [2]	Alkali halides	Qualitative description of avalanche breakdown.
1934	Zener [4]	One-dimension lattice	Field Emission Breakdown; tunneling probability for one-dimension lattice is given.
1937	H. Fröhlich [6]	Alkali halides	Quantitative calculation of the breakdown field; only polar phonons are considered.
1981	M. Sparks et al. [7]	Alkali halides	Quantitative calculation of the laser-induced breakdown field; both polar and nonpolar phonons are included.
1986	E. Cartier et al. (Brown Boveri) [11]	Organic dielectrics (n-C <sub>36</sub> H <sub>74</sub> )	Investigated the transport and relaxation of hot electrons by using electron phonon scattering rates derived from experiments.
1994	D. Arnold et al. (IBM) [1]	SiO <sub>2</sub> thin film	Investigated the transport of hot electrons by Monte Carlo method using electron phonon scattering rates derived from experiments.
2007–2010		GaAs and GaP [8], Si [9], Graphene [10]	Electron phonon scattering rates are calculated from first principles.
2012	Y. Sun et al. [12]	Covalently and ionic bonded inorganic crystals	First principle computations of intrinsic breakdown based on an average electron model and von Hippel's low energy criterion, which agree well with published data.

the first electron through impact ionization, and the repetition of impact ionization until the electron concentration is sufficient to damage the material.

#### *Von Hippel's Low Energy vs. Fröhlich's High Energy Criterion*

As stated above, von Hippel's low energy criterion for avalanche breakdown is that the energy gain from the electric field must be greater than the energy loss to phonons for all energies from the conduction band minimum (CBM) to the threshold for impact ionization. The physical basis of this criterion is that (1) when the electron energy reaches the threshold for impact ionization, one electron with the impact ionization energy will be replaced by two electrons at the CBM, and the process can repeat leading to electron multiplication, avalanche formation, and breakdown and (2) that if the energy loss to phonons is greater than the energy gain from the electric field for any electron energy between the CBM and the impact ionization energy, electrons will collect at that energy and never reach the energy required for impact ionization. Von Hippel's criterion is consistent with an average electron model, as his criterion does not depend explicitly on the tails of the electron energy distribution.

Fröhlich's high energy criterion is based on the high energy tail of the electron energy distribution which, quite logically, should precipitate breakdown. As a result, he requires only that the energy gain from the electric field be greater than the energy loss for phonons for electrons in the high energy tail of the electron energy distribution. Since Fröhlich's breakdown criterion depends explicitly on the high energy tail of the electron energy distribution, it is not consistent with an average electron model, which makes it more complex, whether approached analytically or numerically.

In essence, Fröhlich's theory rests on the assumption that when the breakdown field is reached, the peak of the electron

energy distribution function is well below the ionization energy but possesses a high energy tail which extends to the ionization energy. The behavior of the electrons in the high energy tail determines breakdown. Based on the assumption that only longitudinal polarization waves interact with the electrons, Fröhlich employed quantum mechanics to derive the electron relaxation time for alkali halides based on electron interaction with only longitudinal polarization waves, i.e., longitudinal optical phonons. Fröhlich's quantitative calculation of the breakdown field for alkali halides based on the balance between electron energy gain and energy loss agrees well with experimental data from von Hippel. Figure 1 shows a schematic of von Hippel's low energy and Fröhlich's high energy criteria [13]. The red lines

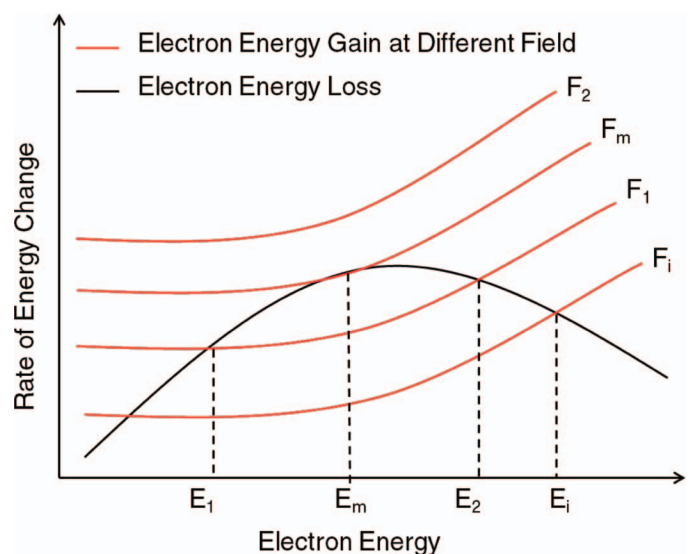


Figure 1. Schematic of von Hippel's low energy and Fröhlich's high energy criteria [13].

represent the rate of energy transfer from the electric field to electrons as a function of electron energy and applied field  $F$ , while the black line represents the rate of energy loss to phonons as a function of electron energy  $E$ .

When the electric field,  $F$ , is sufficiently low, i.e.,  $F_1$  in Figure 1, the energy gain and loss balance at two electron energies,  $E_1$  and  $E_2$ . However, as the field increases, a field of  $F_m$  is reached where the two solutions merge into one  $E_m$ . For higher values of the field, e.g.,  $F_2$ , no solution exists. Thus if  $F > F_m$ , the energy gain will be larger than the energy loss for all  $E$  so that every free electron will increase its energy to the threshold of impact ionization. This led von Hippel to define  $F_m$  as the breakdown field.

Following Fröhlich, even if  $F < F_m$ , equilibrium is not possible. Consider an electron in field  $F_1$ , for which two solutions are possible. Solution  $E_1$  represents a stable equilibrium, while  $E_2$  is unstable, since for  $E > E_2$ , electron energy increases indefinitely. Suppose that the energy for ionization ( $E_i$ ) is such that  $E_2 > E_i$ , in which case the electrons which have energies in excess of  $E_2$  can ionize lattice atoms and thus reduce their energy. However, if  $E_2 < E_i$ , electrons with energy interval  $E_2$  to  $E_i$  will increase their energy on average which results in a continuous increase in the total energy of the electron system, and steady state is impossible. Thus the maximum field for a steady state (i.e., the “critical” field) corresponds to  $E_2 = E_i$ . Once electrons achieve energies in excess of  $E_2$ , they can accelerate rapidly to energies of order  $E_i$ . Perhaps the best that can be said of Fröhlich’s high energy criterion is that it provides a lower limit for fields which give appreciable ionization, while the intrinsic breakdown field is determined by the degree of ionization which is required to produce avalanche breakdown.

### *Spark’s Model With Energy Diffusion*

In 1981, Sparks proposed an average electron model based on avalanche breakdown theory which agrees well with laser induced breakdown data for alkali halides, as noted above [7]. The good agreement is obtained as a result of improved magnitudes and energy dependences of the electron phonon relaxation frequencies, e.g., the contributions of both optical and acoustic phonons to electron energy loss and diffusion in energy space are included. The breakdown field is calculated by solving an eigenvalue equation obtained from a diffusion transport equation in energy space, i.e., in Sparks’ model, electron energy gain from the field and loss to phonons contributes to diffusion of electron energy in a classical approximation, the instability of which indicates breakdown.

The limitations of the average electron model stem both from the difficulty of treating the energy dependence of energy gain and loss properly, and from the neglect of electron diffusion in energy space. Holway and Fradin [14] demonstrated that avalanche breakdown cannot be truly an “average electron” phenomenon. Breakdown can occur without an electric field that, on average, causes every electron below the ionization energy to gain energy. An electron typically gains energy over part of the energy range by diffusion to greater energy while, on average, electrons lose more energy than they gain. Spark’s energy diffusion model is a classical approach to approximating the effect

of electron–phonon interaction on the electron energy distribution.

The simple crystal structure of alkali halides allows an analytical solution of electron relaxation time (the reciprocal of which is electron–phonon scattering rate) and electron energy loss rate. Sparks derived an analytical solution for both of these parameters by treating the contribution of both polar (longitudinal optical phonons) and nonpolar (acoustical and transverse optical phonons) phonons to electron–phonon scattering. Inaccuracy of the theoretical calculation may stem from various approximations made in order to obtain these analytical expressions. The greatest limitation of Sparks’ model is that the analytical expression for electron relaxation time and energy loss rate is derived only for alkali halides and cannot be extended to other more complex materials, which makes the theoretical investigation of many technically important materials (such as SiO<sub>2</sub> and PE) impossible.

### *First Principle Computations of Intrinsic Breakdown*

While both von Hippel and Fröhlich demonstrated great physical insight, they could not conduct reasonably accurate computations of intrinsic breakdown, as the accurate, quantum mechanical–based computations of electron–phonon interactions cannot be executed analytically, and computers were not yet available. With the relatively recent development of computational quantum mechanics based on density functional theory, we can now undertake such computations numerically with reasonable accuracy. Density functional theory (DFT) is based on two theorems. The first says that knowing the electron density is equivalent to knowing the solution to Schrödinger’s equation. The second says that the correct electron density distribution minimizes the total energy. These two theorems provide the basis for a very successful branch of computational quantum mechanics. While DFT is, in principle, exact, numerous approximations are required during practical implementation. Examples include the pseudopotential approximation to combine the effects of the nucleus and the core electrons, and the exchange–correlation approximation to capture the quantum mechanical part of electron–electron interactions.

Electron–phonon interactions, both polar and nonpolar, can be computed using density function perturbation theory (DFPT). While electron density is the central quantity in DFT, first-order changes to the charge density in response to an external perturbation are the central quantity in DFPT. In the present application, the atomic positions are perturbed in a manner characteristic of each phonon mode, which changes the electron density distribution with which an electron interacts. In polar materials, the interaction of an electron with a macroscopic electrical field caused by Coulomb interactions must be calculated in addition to the change to electron density by atomic displacements characteristic of each phonon mode. Computation of the electron–phonon interactions is cumbersome for two reasons. First, accurate evaluation of electron–phonon scattering rate requires a very dense sampling of both the electronic ( $k$ ) and the phononic ( $q$ ) reciprocal space grids, significantly more dense than required in standard DFT. Second, the number of phonon modes is  $3N$ , where  $N$  is the number of atoms in the system. If the unit

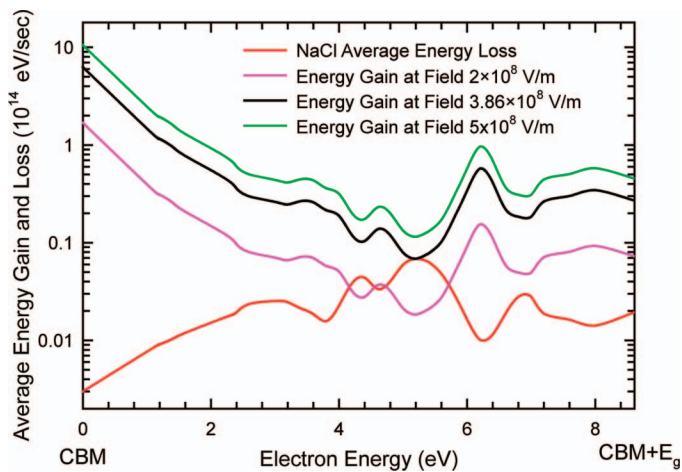


Figure 2. The average energy loss and energy gain at electric fields of  $2 \times 10^8$  V/m,  $3.86 \times 10^8$  V/m, and  $5 \times 10^8$  V/m for NaCl as a function of electron energy. The electron energy scale is referenced to the conduction band minimum (CBM). The intrinsic breakdown field of NaCl is estimated as the electric field for which the energy gain curve (black solid line) is greater than energy loss curve (red line) for all electron energies from the CBM to  $8.61$  eV above CBM, i.e., from the CBM to the CBM plus the bandgap ( $E_g$ ) of NaCl.

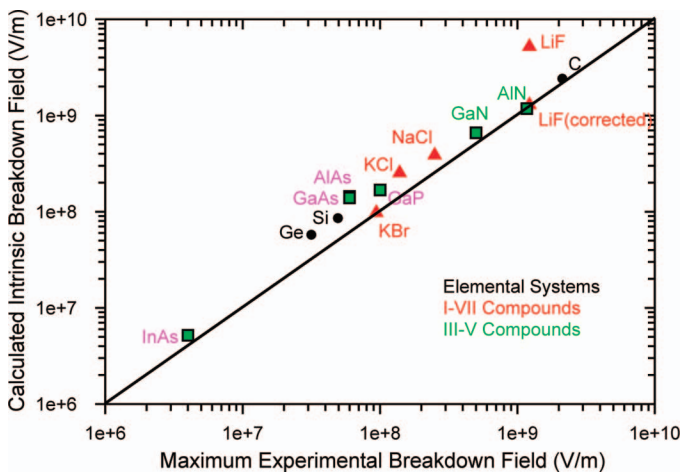


Figure 3. Comparison of the maximum experimental breakdown field and the calculated intrinsic breakdown field for a range of covalently bonded and ionic materials. The data are tabulated in Table 2. In the case of LiF, the enthalpy of formation ( $6.39$  eV) is much lower than the bandgap ( $14.2$  eV). Thus bond breakage will occur before impact ionization. The LiF (corrected) represents our result when the enthalpy of formation is used as impact ionization threshold instead of the bandgap. The symbols code for material type (element, etc.) while the text in the figures codes for material structure, i.e., (black) Diamond Structure: Ge, Si, C; (red) Rocksalt Structure: KBr, KCl, NaCl, LiF; (purple) Zincblende Structure: InAs, GaAs, GaP, AlAs; (green) Wurtzite Structure: AlN, GaN.

cell of the material has a limited number of atoms, this process is practical and can be used with periodic boundary conditions to model a bulk material. For materials with large unit cells, such as polypropylene, computation for all the phonon modes is very time consuming.

The electron energy gain from the field is easily expressed, although the effective electron mass is a function of electron energy and must be approximated. The electron–phonon coupling matrix, which gives the probability of an electron scattering from an initial state,  $i$ , to a final state,  $j$ , through interaction with a phonon mode  $\alpha$ , must be calculated using DFPT and provides the basis for computing electron energy loss to phonons. Providing any mathematical description of these phenomena would result in many very complex equations, which have been published in [12]. We will therefore restrict the discussion to the conceptual basis of the computations.

Once the electron–phonon scattering rate as a function of electron energy has been computed, the energy loss as a function of electron energy can be calculated, shown as the red line of Figure 2. The energy gain from the electric field is reasonably easy to compute and is also shown in Figure 2 for several electric fields. The breakdown field is determined by the condition that the energy gain is greater than the energy loss up to the energy threshold for impact ionization (i.e., the bandgap) which is  $8.61$  eV for NaCl. In the case of NaCl shown in Figure 2, the computed breakdown field is about  $3.86 \times 10^8$  V/m.

Figure 3 compares our computations with literature data for the intrinsic breakdown of many materials we have addressed to date. The data include elemental systems: Ge, Si, C (diamond cubic structure); I-VII compounds: KBr, KCl, NaCl, LiF (rocksalt structure); III-V compounds: InAs, GaAs, GaP, AlAs (Zincblende Structure), and AlN, GaN (Wurtzite Structure). The groups of materials are represented by differing symbols in Figure 3. A major difficulty in obtaining agreement between theory and experiment for the intrinsic breakdown field is determining whether the experimental data represent intrinsic breakdown. Breakdown fields from the literature for a given material vary substantially as a result of material defects and the experimental technique employed. The maximum breakdown field from reported data provides the best estimate of intrinsic breakdown strength. We note that the computed  $F_{bd}$  value represents the upper bound for intrinsic breakdown field. The best available breakdown data for alkali halides are generated by optical breakdown measurements, which eliminate the influence of many extraneous factors such as electrode effects, interfaces, etc.

The case of LiF (Figure 3) is interesting. If we use the usual criterion for breakdown, that the energy gain is everywhere greater than the energy loss from the CBM to the CBM plus the bandgap, we predict much too great an intrinsic breakdown. However, the enthalpy of formation for LiF is much less than the bandgap so that failure is likely to occur from bond breakage. When the enthalpy of formation is used in place of the bandgap, the computed intrinsic breakdown agrees very well with the measured data as represented by LiF (corrected) in Figure 3.

The ability to compute intrinsic breakdown with reasonable accuracy on a first principles, parameter-free basis is gratifying; however, such computations remain somewhat cumbersome.

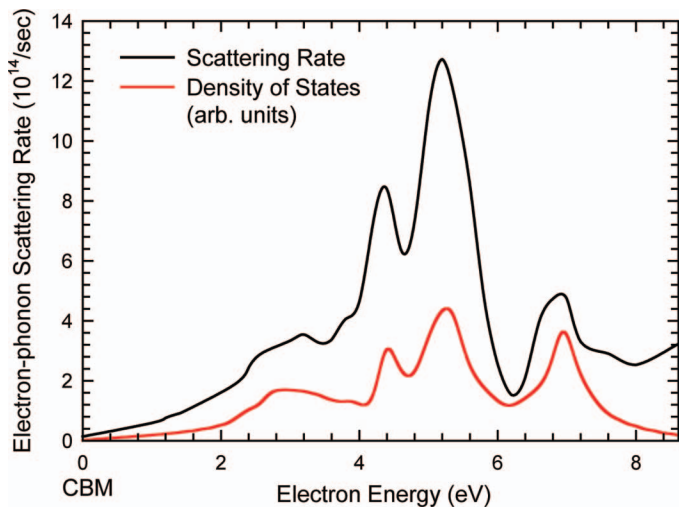


Figure 4. The electron–phonon scattering rate and the density of states for NaCl at room temperature as a function of electron energy. The electron energy scale is referenced to the conduction band minimum (CBM).

Accurate evaluation of electron–phonon scattering rates requires a very dense sampling of both the electronic and the phononic reciprocal space grids, significantly more dense than required in

standard DFT computations. However, we can use such computations to look for correlations between basic material properties and intrinsic breakdown. Not surprisingly, intrinsic breakdown depends on the electron–phonon scattering rate, which is the main mechanism for electron energy loss. The electron–phonon scattering rate tends to follow the electron density of states, as seen in Figure 4. Thus a peak in the density of states within the energy range of interest (CBM to CBM + the bandgap,  $E_g$ ) tends to increase the breakdown field as seen in Figure 2.

In order to develop an intuition for the fundamental chemical and physical factors that control intrinsic breakdown, we examined the correlation of several easily computable attributes with the computed  $F_{bd}$  values. Our results indicate a clear correlation between  $F_{bd}$  and the material bandgap and the highest phonon frequency (i.e., the phonon cutoff frequency). As seen from Table 2, the breakdown strength tends to increase with bandgap and phonon cutoff frequency. The phonon cutoff frequencies are calculated from DFPT, while the bandgap is the experimental value from the literature. The dependence of intrinsic breakdown with these parameters is understandable intuitively, as a material with a greater bandgap will display a higher threshold for impact ionization, and materials with greater phonon cutoff frequency tend to have greater average energy loss during each electron–phonon scattering event which leads to larger  $F_{bd}$  values. Figures 5 and 6 show plots of calculated intrinsic

**Table 2. For All Systems Studied Here, the Calculated Highest Phonon Frequency (in THz) and the Breakdown Field (in V/m) as per von Hippel’s Criterion Are Listed. The Experimental Bandgap (in eV), the Highest Observed Breakdown Field (in V/m), and the Method Adopted in Such Measurements Are Also Listed. The Computed LiF Intrinsic Breakdown Is Shown Based on the Bandgap Criterion, While the LiF (corrected) Value Is Based on the Bond Energy Criterion.**

	Phonon cutoff frequency (THz)	Calculated intrinsic $F_{bd}$ (V/m)	Exp. $E_g$ (eV)	Exp. $F_{bd}$ (V/m)
Ge	8.73	$5.64 \times 10^7$	0.74 [15]	<sup>a</sup> $3.2 \times 10^7$ [21]
Si	15.3	$8.39 \times 10^7$	1.17 [15]	<sup>a</sup> $5 \times 10^7$ [22]
C	37.9	$2.37 \times 10^9$	5.48 [15]	<sup>b</sup> $2.15 \times 10^9$ [23]
KBr	5.23	$9.75 \times 10^7$	7.81 [16]	<sup>c</sup> $9.4 \times 10^7$ [24]
KCl	6.88	$2.53 \times 10^8$	8.51 [16]	<sup>c</sup> $1.39 \times 10^8$ [24]
NaCl	8.13	$3.86 \times 10^8$	8.61 [16]	<sup>c</sup> $2.5 \times 10^8$ [7]
LiF	19.8	$5.2 \times 10^9$	14.2 [15]	<sup>b</sup> $1.22 \times 10^9$ [25]
LiF (corrected)	19.8	$1.29 \times 10^9$	14.2 [15]	<sup>b</sup> $1.22 \times 10^9$ [25]
AlAs	11.8	$1.44 \times 10^8$	2.17 [17]	<sup>a</sup> $6 \times 10^7$ [17]
GaAs	8.82	$1.39 \times 10^8$	1.43 [18]	<sup>a</sup> $6 \times 10^7$ [18]
GaP	12.2	$1.68 \times 10^8$	2.26 [19]	<sup>a</sup> $1.0 \times 10^8$ [19]
InAs	7.73	$5.19 \times 10^6$	0.354 [19]	<sup>a</sup> $4 \times 10^6$ [19]
AlN	27.6	$1.18 \times 10^9$	6.23 [20]	<sup>a</sup> $1.17 \times 10^9$ [26]
GaN	23.3	$6.6 \times 10^8$	3.2 [15]	<sup>a</sup> $5 \times 10^8$ [19]

<sup>a</sup>Electrical breakdown.

<sup>b</sup>1.06- $\mu$ m laser breakdown.

<sup>c</sup>10.6- $\mu$ m laser breakdown.

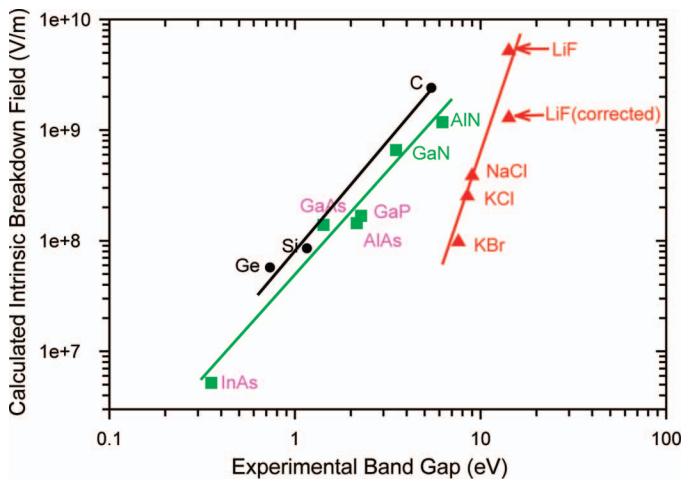


Figure 5. Correlation between the calculated intrinsic breakdown field and the experimental bandgap. Different correlation lines are formed for different groups of materials as indicated by different symbols in the figure.

breakdown as a function of these two parameters from which we see that three different correlation lines are formed for differing material groups, although the power law dependence appears to differ, i.e., covalently bonded elements (Ge, Si, and C), III-V compound semiconductors (InAs, GaAs, GaP, AlAs, AlN, GaN), and ionic bonded alkali halides (KBr, KCl, NaCl, LiF).

For a given bandgap, covalently bonded materials (Ge, Si, and C) have the greater breakdown strength, while for a given phonon cutoff frequency, ionic materials (alkali halides) have the greater breakdown strength. Electron-phonon interaction is stronger in an ionic (polar) material than in a nonpolar material which probably accounts for effect of phonon cutoff frequency. All the ionic materials have very large bandgap, and the breakdown strength increases very rapidly ( $\sim 4$ th power) with the bandgap. The covalently bonded materials, which tend not

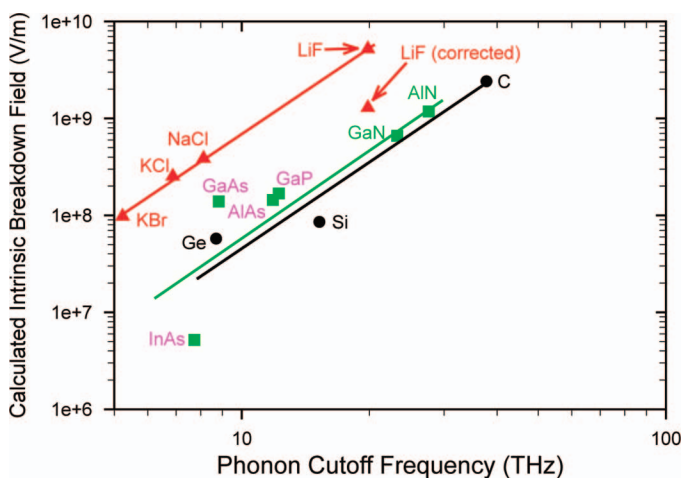


Figure 6. Correlation between the calculated intrinsic breakdown field ( $F_{bd}$ ) and the phonon cutoff frequency. Different correlation lines are formed for different groups of materials as indicated by different symbols in the figure.

to be polar, have a greater range of bandgap, and the intrinsic breakdown field increases roughly as the square of the bandgap. The ionic materials tend to have lower phonon cutoff frequency than do the covalent materials, but the intrinsic breakdown field increases more rapidly with cutoff frequency, probably because the ionic materials have strong interactions with a wider range of phonons, i.e., both polar and nonpolar, while the covalent materials have greater phonon cutoff frequency but the breakdown strength increases less rapidly with cutoff frequency, probably as a result of the reduced electron-phonon coupling in such materials.

## Conclusion

The basic quantum mechanical theory for intrinsic breakdown was developed by von Hippel and Fröhlich over 70 years ago, but only now can we exploit their ideas accurately through the use of computational quantum mechanics. As shown above, von Hippel's low energy criterion for intrinsic breakdown provides remarkably good agreement with measured data for a range of both ionic and covalently bonded materials. We can correlate intrinsic breakdown with both bandgap and phonon cutoff frequency, although the relationships differ for different groups of materials.

The challenge going forward is to move from intrinsic breakdown to engineering breakdown through inclusion of effects caused by morphology, chemical impurities (impurity states in the bandgap), and defects such as nanocavities. We believe that inclusion of these phenomena is possible using Monte Carlo computations with parameters computed using first principles methods, and we are pursuing this approach.

## References

- [1] D. Arnold, E. Cartier, and D. J. Dimaria, "Theory of high-field electron transport and impact ionization in silicon dioxide," *Phys. Rev. B*, vol. 49, pp.10278–10297, 1994.
- [2] A. von Hippel, "Electric breakdown of solid and liquid insulators," *J. App. Phys.*, vol. 8, pp. 815–832, 1937.
- [3] F. Seitz, "On the theory of electron multiplication in crystals," *Phys. Rev.*, vol. 76, pp. 1376–1393, 1949.
- [4] C. M. Zener, "A theory of the electrical breakdown of solid dielectrics," *Proc. Roy. Soc.*, 145, pp. 523–529, 1934.
- [5] R. C. Buehl and A. von Hippel, "Electric breakdown. Strength of ionic crystals as a function of temperature," *Phys. Rev.*, vol. 56, pp. 941–947, 1939.
- [6] H. Frohlich, "Theory of electrical breakdown in ionic crystals," *Proc. Roy. Soc.*, 160, pp. 230–241, 1937.
- [7] M. Sparks, D. L. Mills, R. Warren, T. Holstein, A. A. Maradudin, L. J. Sham, E. Loh Jr., and D. F. King, "Theory of electron-avalanche breakdown in solids," *Phys. Rev. B*, vol. 24, pp. 3519–3536, 1981.
- [8] J. Sjakste, N. Vast, and V. Tyuterev, "Ab initio method for calculating electron-phonon scattering times in semiconductors: Application to GaAs and GaP," *Phys. Rev. Lett.*, vol. 99, pp. 236405-1-4, 2007.
- [9] O. D. Restrepo, K. Varga, and S. T. Pantelides, "First-principles calculations of electron mobilities in silicon: Phonon and Coulomb scattering," *Appl. Phys. Lett.*, vol. 94, pp. 212103-1-3, 2009.
- [10] K. M. Borysenko, J. T. Mullen, E. A. Barry, S. Paul, Y. G. Semenov, and J. M. Zavada, "First-principles analysis of electron-phonon interaction in graphene," *Phys. Rev. B*, vol. 81, pp.121412 (R) -1-4, 2010.
- [11] E. Cartier and P. Pfluger, "Transport and relaxation of hot conduction electrons in an organic dielectric," *Phys. Rev. B*, vol. 34, no. 12, pp. 8822–8827, 1986.
- [12] Y. Sun, S. A. Boggs, and R. Ramprasad, "The intrinsic electrical breakdown strength of insulators from first principles," *Appl. Phys. Lett.*, vol. 101, pp. 132906-1-5, 2012.

- [13] R. Stratton, *Progress in Dielectrics*, vol. 3, J. B. Birks and J. Hart, Ed. New York, NY: Wiley, 1961, pp. 235–292.
- [14] L. H. Holway and D. W. Fradin, “Electron avalanche breakdown by laser radiation in insulating crystals,” *J. App. Phys.*, vol. 46, no. 1, pp. 279–291, 1975.
- [15] F. Tran and P. Blaha, “Accurate band gaps of semiconductors and insulators with a semilocal exchange-correlation potential,” *Phys. Rev. Lett.*, vol. 102, pp. 226401-1-4, 2009.
- [16] R. T. Poole, J. G. Jenkin, J. Liesegang, and R. C. G. Leckey, “Electronic band structure of the alkali halides. I. Experimental parameters,” *Phys. Rev. B*, vol. 11, pp. 5179–5189, 1975.
- [17] Yu. A. Goldberg, “Ternary and quaternary III-V compounds,” in *Handbook Series on Semiconductor Parameters*, vol. 2, M. Levinstein, S. Rumyantsev, and M. Shur, Ed. London, UK: World Scientific, chapter 1.
- [18] M. N. Yoder, “Wide bandgap semiconductor materials and devices,” *IEEE Trans. Electron Devices*, vol. 43, pp. 1633–1636, 1996.
- [19] NCSR: National Compound Semiconductor Roadmap. Available: [www.ncsr.csci.va.com](http://www.ncsr.csci.va.com).
- [20] I. Vurgaftman and J. R. Meyer, “Band parameters for III–V compound semiconductors and their alloys,” *J. Appl. Phys.*, vol. 89, pp. 5815–5875, 2001.
- [21] S. L. Miller, “Avalanche breakdown in germanium,” *Phys. Rev.*, vol. 99, pp. 1234–1241, 1955.
- [22] J. N. Park, K. Rose, and K. E. Mortenson, “Avalanche breakdown effects in near intrinsic silicon and germanium,” *J. Appl. Phys.*, vol. 38, pp. 5343–5351, 1967.
- [23] P. Liu, R. Yen, and N. Bloembergen, “Dielectric breakdown threshold, two-photon absorption, and other optical damage mechanisms in diamond,” *IEEE J. Quantum Electron*, vol. QE-14, no. 8, pp. 574–576, 1978.
- [24] E. Yablonoitch, “Optical dielectric strength of alkali halide crystals obtained by laser induced breakdown,” *Appl. Phys. Lett.*, vol. 19, pp. 495–497, 1971.
- [25] W. L. Smith, J. H. Bechtel, and N. Bloembergen, “Dielectric-breakdown threshold and nonlinear-refractive-index measurements with picosecond laser pulses,” *Phys. Rev. B*, vol. 12, pp. 706–714, 1975.
- [26] T. P. Chow, “SiC and GaN high-voltage power switching devices,” *Materials Science Forum*, vol. 338–342, pp. 1155–1160, 2000.

**Ying Sun** received her bachelor’s and master’s degrees in electrical engineering from Xi’an Jiaotong University in 2006 and 2009, respectively. She is presently pursuing a PhD in Materials Science at the University of Connecticut, which she expects to complete in 2013.

**Clive Bealing** received his bachelor’s and PhD degrees in physics, both from King’s College London in 2006 and 2010, respectively. He then joined the Department of Materials Science and Engineering at Cornell University as a postdoctoral associate. He joined the University of Connecticut’s Institute of Materials Science in 2012, where he is currently pursuing theoretical research into breakdown and aging phenomena in dielectric materials.

**Steven Boggs** (F ’92) was graduated with a BA from Reed College in 1968 and received the PhD and MBA degrees from the University of Toronto in 1972 and 1987, respectively. He spent 12 years with the Research Division of Ontario Hydro, Canada. He was elected an IEEE Fellow for his contributions to understanding of SF<sub>6</sub>-insulated systems. From 1987 to 1993, he was Director of Research and Engineering at Underground Systems, Inc. He is presently Director of the Electrical Insulation Research Center and Research Professor of Materials Science, Electrical Engineering, and Physics at the University of Connecticut. In 2010, he received the IEEE Thomas W. Dakin Award.

**Ramamurthy Ramprasad** was graduated from the Indian Institute of Technology, Madras, India, with a BTech in metallurgical engineering and from the University of Illinois, Urbana-Champaign, with a PhD in materials science and engineering. After six years at Motorola, Inc., where he worked on problems related to field emission for flat panel display applications, advanced dielectric and magnetic materials, and metamaterials for RF and microwave applications, he joined the Department of Materials Science and Engineering at the University of Connecticut as a faculty member. Dr. Ramprasad’s area of expertise is in the first principles modeling of materials using density functional theory. He is the author of about 80 peer-reviewed journal papers, numerous invited presentations and conference papers, and four issued patents.

